LANGMUIR

pubs.acs.org/Langmuir Article

Tip Streaming of a Lipid-Stabilized Double Emulsion Generated in a Microfluidic Channel

Kristian Torbensen, Charles N. Baroud, Sandra Ristori, and Ali Abou-Hassan*

Cite This: *Langmuir* 2021, 37, 7442−7448 Read Online

ACCESS | Metrics & More | Article Recommendations | Supporting Information

ABSTRACT: Water/oil/water (w/o/w) double emulsions (DEs) are multicompartment structures which can be used in many technological applications and in fundamental studies as models of cell like microreactors or templates for other materials. Herein, we study the flow dynamics of water/oil/water double emulsions generated in a microfluidic device and stabilized with the phospholipid 1,2-dimyristoyl-*sn*-glycero-3-phosphocholine (DMPC). We show that by varying the concentration of lipids in the oil phase (chloroform) or by modulating the viscosity of the aqueous continuous phase, the double emulsions under flow exhibit a rich dynamic behavior. An initial deformation of the double emulsions is followed by tube extraction at the rear end, relative to the flow direction, resulting in pinch off at the tube extremity by which small aqueous compartments are released. These compartments are phospholipid vesicles as deduced from fluorescence experiments. The overall process can thus be of help to shed light on the mechanical aspects of phenomena such as the budding and fusion in cell membranes.

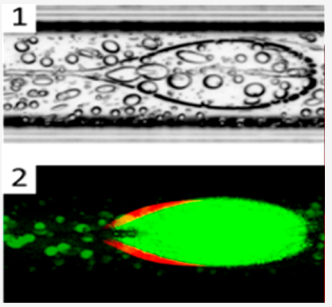

INTRODUCTION

Over recent decades, the field of droplet microfluidics has witnessed a rapid evolution.[1,2] This is, in particular, due to achievements in soft lithographic technology[3] and in engineering simple and versatile microfluidic devices built using coaxially aligned capillary tubes.[4,5] With high control over flow rates and both channel geometry and dimensions, monodisperse multicompartment droplets with single or multiple cores can be generated with high throughput for applications in biology, chemistry, and nanotechnology.[6−9] Water/oil/water double emulsions (DEs) are droplets that have attracted widespread interest over about 30 years for applications ranging from the formulation of pharmaceutics to more fundamental studies.[4,10−12] They can be generated with a narrow size distribution using the two-step emulsification method in microfluidics.[10] The DEs are used as templates for the preparation of other materials including, among others, giant phospholipid vesicles,[13−15] polymersomes,[16,17] and hole−shell particles[18] or as a model of microreactors for the synthesis of biomaterials[13] and the study of complex biological processes.[19−22]

Several studies on deformation, breakup, and/or tip streaming of single emulsions in flow systems have been reported[8,23−25] but less on DEs. While the behavior of single emulsions can be described by the interfacial tension and the viscosity ratio between the droplet and the continuous flowing outer fluid, the flow dynamics of multiple emulsions require several additional parameters to account for multiple interfaces and the presence of domains with different viscosities.[8] We must therefore keep track of the viscosities (μ) of the three phases, the inner phase (μ_{in}), the middle oil phase (μ_{oil}), and the external continuous phase (μ_{ext}), as well as the value of the interfacial tension (γ), which we will consider to be the same on both interfaces.

When subject to stress, such as under shear flow conditions in microfluidic channels, deformation of both the core droplet and the shell might occur, either independently or simultaneously. The dynamics of double emulsions under shear flow has been investigated numerically by Hua et al.[26] and both numerically and experimentally by Chen et al.[27,28] in a Couette geometry. The deformation of the outer droplet (i.e., the middle phase) was shown to be governed by competition between viscous shear stress and interfacial tensions together with the ratio between the core and the outer droplet radii. The deformation of the core was demonstrated to be mainly induced by a vorticity flow within the outer droplet, generated by the shear stress between the middle phase and the external phase. It was furthermore shown[27] that at critical capillary numbers, a transformation from a steady shape to a transient deformation eventually resulted in the breakup of the outer droplet. Ma et al.[29] investigated the core deformation of w/o/w DEs under sheath flow focusing. They emphasized the significance of core and shell viscosities on core deformation, whereas the type of surfactant present at the interfaces apparently was of minor importance. Chunfeng et al.[30] and Tao et al.[31] numerically studied the flow dynamics of

Received: March 24, 2021
Revised: May 24, 2021
Published: June 10, 2021

https://doi.org/10.1021/acs.langmuir.1c00827
Langmuir 2021, 37, 7442−7448

compound drops in contracting tubes. Similarly, Chen et al.[32] investigated the deformation and breakup mechanism of double emulsions in a tapered nozzle.

In this manuscript, we show that DMPC stabilized DEs elaborated with chloroform as the oil shell exhibits a rich dynamic behavior under flow in a microfluidic channel. Depending on the concentration of DMPC in the oil shell and the concentration of poly(vinyl alcohol) (PVA) in the continuous phase, a tube can be expelled from the rear of the DEs by tip streaming from which smaller daughter droplets are ejected. We imaged the dynamic process of DE formation using bright field and fluorescence microscopy inside and at the exit of the channel. Our results show that stable DEs can be generated using such a method, and the daughter droplets are aqueous compartments stabilized by DMPC. To the best of our knowledge, this is the first demonstration on tip streaming using phospholipids as a surfactant, which points out the major role played by a bilayer rather than a single layer to act as a limit surface and improves the possible comparison with cell-like compartments.

MATERIALS AND METHODS

Chemicals. Chloroform, poly(vinyl alcohol) (PVA, M_w 18 kDa), α-hemolysin, and fluorescein were supplied by Sigma-Aldrich. DMPC was supplied by Lipoids, Inc. L-α-Phosphatidylethanolamine-*N*-(lissamine rhodamine B sulfonyl) (ammonium Salt) was supplied by Avanti Polar Lipids. All chemicals were used as received.

Double-Emulsion Generation. The double emulsions were generated using a microfluidic flow focusing device consisting of coaxially aligned glass capillary tubes assembled using commercially available fittings, i.e., T-crosses and ferrules. The absence of any glued sealing not only enables a fast assembly procedure but also provides the opportunity of fast replacement of clogged or damaged capillary tubes. The microfluidic device consists of coaxially aligned glass tubes of various dimensions and geometry. First, polyimide-coated 365/75 μm (outer diameter [o.d.]/inner diameter [i.d.]) glass capillary tubes (Polymicro) are inserted into a cylindrical 1/0.5 mm (o.d./i.d.) borosilicate tube (Drummond Scientific). The borosilicate tube was narrowed in one end for enhanced flow focusing by exposing the tube orifice to a butane flame while rotating the tube. The inner wall and the orifice of this tube were rendered hydrophobic using 2% (v/v) trichloro(1*H*,1*H*,2*H*,2*H*-perfluorooctyl)silane (Sigma-Aldrich) in toluene, rinsed with toluene, and dried overnight at 70 °C to obtain the desired wetting properties. These tubes are in turn inserted into a square borosilicate tube with dimensions of 1.25 × 1 mm (outer/inner side length, Vitrocom). A second cylindrical borosilicate tube, likewise flame treated and serving as the DE collector tube, was inserted from the opposite end of the square tube, and the two cylindrical tubes were positioned with the narrowed orifices within a close distance, followed by positioning of the two innermost fused capillary tubes close to the orifice of the left cylindrical tube. All glass tubes were assembled using T-crosses (P-727, Upchurch Scientific), ferrules (F-331, Upchurch Scientific), and pieces of 1/3 mm (o.d./i.d.) silicon tubing (Tygon Versilic Silicon Tubing, Sigma-Aldrich) and mounted on a Plexiglas stand. A more thorough description of this microfluidic device has been published elsewhere.[33]

Bright Field and Fluorescence Imaging. A Zeiss Axiovert 200 microscope mounted with a NeoFluar objective (2.5× magnification and field depth of 62.4 μm) and a Dasla CCD camera was employed for monitoring the DEs. For monitoring the fluorescent probes, a FluoArc laser was connected to the microscope, and the appropriate wavelengths were selected with optical band-pass filters (532 nm for rhodamine B and 445 nm for fluorescein). Bright field images were recorded with 300 frames/s with an exposure time of 3000 μs. Dynamic fluorescence images were recorded with 100 frames/s with an exposure time of 9000 μs. Static fluorescence images were recorded with 10 frames/s with an exposure time of 100 ms. Freely available software ImageJ was used for image processing.

Interfacial Tension Measurements. An interfacial tensiometer (DSA100, Krüss GMBH), mounted with a 0.516 or 1.837 mm needle, was used for measuring the interfacial tension between oil and aqueous phases, employing the pendant drop method with the oil phase suspended in the aqueous phase.

Viscosity Measurements. Viscosities of the PVA solutions were measured using an Anthon Paar Automated Micro Viscometer, employing the rolling ball method, using a 1.6 mm capillary tube for the 2% PVA solution and a 1.8 mm capillary tube for 5−10% solutions. Rolling time was 10 s. The measured viscosity values were found to be 1.63, 3.62, 6.97, and 12.94 mPa·s for 2%, 5%, 7.5%, and 10% PVA, respectively, see Figure S4.

α-Hemolysin Studies. α-Hemolysin (Sigma-Aldrich) was incorporated in the DMPC membranes by collecting the double emulsions on a glass slide mounted with a silicon reservoir filled with an aqueous 2% PVA solution and α-hemolysin at a concentration of 50 μg/mL.

RESULTS AND DISCUSSION

The w/o/w double emulsions studied in this work are generated using a coflow microfluidic channel,[33] as shown in Figures S1 and S2. The oil phase is constituted of pure chloroform supplemented with various concentrations of 1,2-dimyristoyl-*sn*-glycero-3-phosphocholine (DMPC) as the phospholipid (see Materials and Methods and SI for more details). Poly(vinyl alcohol) (PVA) is added to the aqueous phases in order to modify the values of viscosity. The interfacial tensions and viscosities of the different formulations are plotted in Figures S3 and S4, respectively. The measurements indicate that the interfacial tension at the same DMPC concentration is independent of the concentration of PVA, for [PVA] ≥ 1% w/w reaching asymptotic values of 0.27, 0.18, and 0.13 mN·m^{-1} for DMPC concentrations of 0.1%, 0.5%, and 1.0%, respectively. In contrast, PVA can be used to efficiently modify the viscosity of the aqueous phase. The shape of each droplet is determined by a balance between the interfacial and viscous forces, as described by the capillary number Ca = $\mu U/\gamma$, where the parameters are characteristic values of the interfacial tension (γ), the flow velocity (U), and the viscosity (μ). The DE droplets are monitored using bright field and fluorescence microscopy at various positions downstream of the point of confluence in the microfluidic device (Figure S1), where they are formed (Figure S2 and Video 1). Fluorescein is added to the inner aqueous phase in order to visualize the core of the droplet, while rhodamine B-labeled phospholipids are used as dopants of DMPC in order to image the oil shell. Accordingly, the core drops are green, while the red color indicates phospholipids within the oil shell.

The presence and concentration of DMPC have a major influence on the shape of the DE droplets as they flow through the capillary tube, as shown in Figure 1. Indeed, while the droplets flowing in the absence of DMPC showed slight deformation retaining their concentric spherical shapes (top line of Figure 1A and Figure S5), addition of even small quantities of phospholipids leads to a stronger deformation of the oil shell that increases progressively as the droplet travels in the capillary tube downstream of its point of formation (Figure 1B−D). In the absence of DMPC, the droplets of the double emulsion modify their shape to equilibrate the viscous and capillary effects as they flow. This is also the case in the flow of simple droplets or bubbles.[34] However, the transition from these small deformations to the singular shape of the tip streaming requires the presence of the phospholipids. The

https://doi.org/10.1021/acs.langmuir.1c00827
Langmuir 2021, 37, 7442−7448

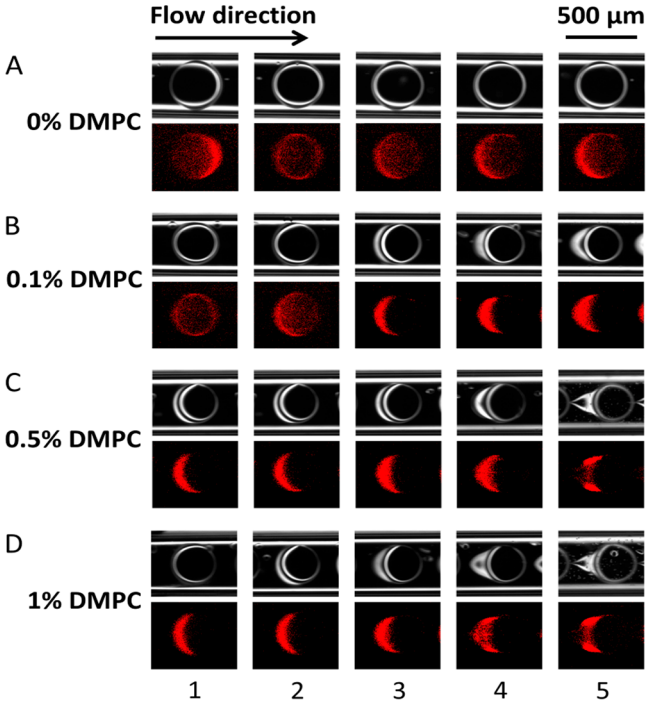

Figure 1. Bright field (top) and fluorescence (bottom) images recorded along the exit tube of the microfluidic device at distances of (1) 0.2, (2) 5.5, (3) 11, (4) 16.5, and (5) 22 mm from the point of droplet formation when 2% w/w PVA is used as an internal and external aqueous phase. Concentrations of DMPC in the oil phase are 0%, 0.1%, 0.5%, and 1% (w/w) in A, B, C, and D, respectively. Inner diameter of the tube is 500 μm. Flow rates applied: Q_1 (H_2O/2% w/w PVA and 0.02% w/w fluorescein, see Figure S5) = 4.17×10^{-4} cm^3 s^{-1}, Q_2 (chloroform/various concentrations of DMPC and 0.02% w/w rhodamine B-labeled phospholipids) = 1.67×10^{-4} cm^3 s^{-1}, and Q_3 (H_2O/2% w/w PVA) = 4.17×10^{-4} cm^3 s^{-1}. Capillary numbers are Ca = 2×10^{-3} for the case for no DMPC, and Ca = 6×10^{-2} for all other cases. Flow direction is from left to right.

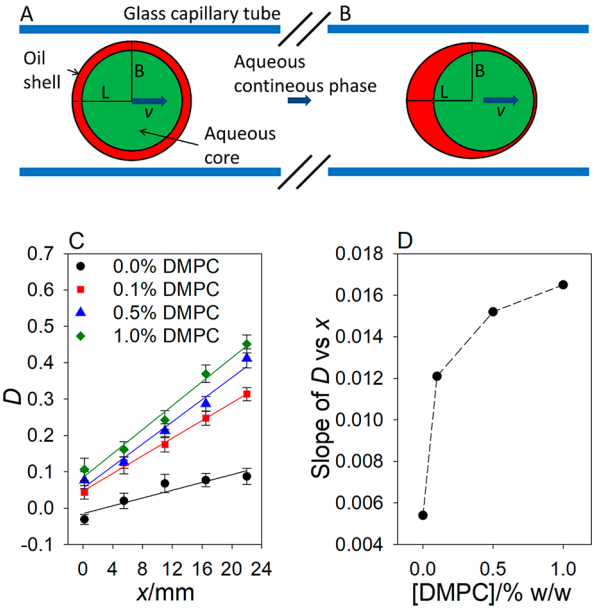

Figure 2. Sketch illustrating the deformation of the middle drop and transport of surfactant herein. (A) B and L are the axial and transverse dimensions, respectively, of the double emulsion moving in the capillary tube with velocity v. (B) Intermediate drop deformation, occurring further down the capillary tube, illustrating the rearrangement of the oil phase, and accumulation of surfactant at the rear of the double emulsion. (C) Plot of the deformation parameter D vs the distance x traveled by the double emulsion. (D) Extent of deformation, expressed as the slope of the lines in A, vs the DMPC concentration. Dashed line in B is a guide to the eye. Reported values are the average of three measurements.

extent of deformation depends on the concentration of DMPC despite the nominal capillary number remaining constant. Instead, the accumulation of DMPC at the rear of the droplets, as shown by the red color on the images, indicates that the interface is not at equilibrium and that this effect depends on the concentration of DMPC. Indeed, the deformation and tip formation become more pronounced as the concentration of DMPC is increased, as shown in Figure 1D, where the outer drop of the DE not only deforms more rapidly but eventually forms a thin tube at the rear of the DE. This accumulation of DMPC molecules at the rear of the droplet is consistent with the classical models of recirculating flows within rectilinear motion, where the interface motion accumulates partially soluble molecules at the rear end.[34] Nonetheless, the ability to fluorescently label the phospholipids provides the first direct evidence that this phenomenon is preserved in the case of double emulsions. Under all these conditions, the aqueous core of the double emulsion remains concentric, as shown in Figure S5.

To quantify the extent of the deformation (before any observed tip streaming), approximated as the transformation of a sphere to an ellipsoid, we adapt the dimensionless index D,[35] defined as $D = (L - B)/(L + B)$, where B and L are the axial and transverse dimensions of the middle droplet (i.e., the oil shell), respectively, as outlined in Figure 2A and 2B. Values for B and L are determined from the bright field images of Figure 1. A linear relationship between D and the distance (x) traveled by the DEs is observed for all of the applied concentrations of the phospholipid, see Figure 2C. This means that a gradual deformation occurs as the droplet advances. The rate of increase of this deformation is plotted in Figure 2D and shows that the deformation rate also increases for higher concentrations of DMPC.

The results of Figures 1 and 2 show that the higher concentrations of DMPC not only lead to larger deformation of the interface but also increase the rate at which the deformation happens. Taken together, these observations are an indication of the depletion of DMPC molecules in the oil phase at the lower DMPC concentrations, while the higher DMPC concentrations maintain a lower global surface tension even as the molecules are swept to the rear of the droplet. This picture, in turn, is suggestive of a saturation threshold for DMPC in the oil phase.

In order to evaluate the relative effect of viscosity change while maintaining the time/space relation as the droplets flow in the channel, the flow rates were kept fixed while the concentration of PVA present in the outer aqueous phase was increased to 5%, 7.5%, or 10%. Increasing the viscosity leads to a higher dripping frequency and consequently a smaller droplet size.[33] The resulting deformations and tip streaming are shown in Figure 3, where the inner water droplets display a much larger deformation than the case of Figure 1. Indeed, the characteristic capillary numbers for these experiments are in the range $1.4–5.0 \times 10^{-1}$, which are large values compared with other typical microfluidic flows, particularly due to the

https://doi.org/10.1021/acs.langmuir.1c00827
Langmuir 2021, 37, 7442−7448

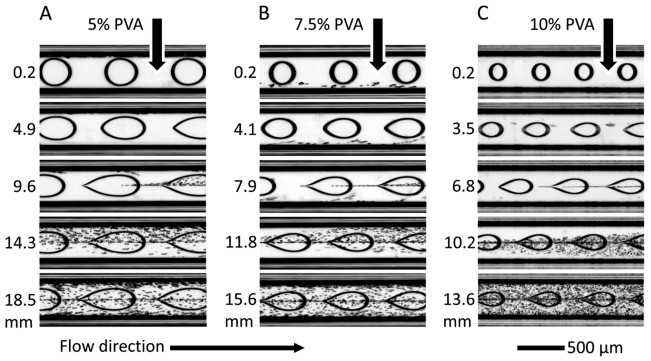

Figure 3. Bright field images showing the gradual deformation of the double emulsion as an effect of the increasing viscosity of the continuous flowing phase. Each column represents the situation obtained with the PVA concentration indicated. Each frame of the columns is recorded at different locations in the capillary tube. Numbers to the left of each column show the event location in the tube at the distance from the point of formation of the double emulsions. Flow direction is from left to right. Flow rates applied: Q_1 (H_2O/2% w/w PVA) = 4.17 × 10^{-4} cm^3 s^{-1}, Q_2 (chloroform/1% w/w DMPC) = 1.67 × 10^{-4} cm^3 s^{-1}, and Q_3 (H_2O/various concentration of PVA) = 4.17 × 10^{-4} cm^3 s^{-1}. Capillary numbers are Ca = 0.14 for the case 5% w/w PVA, Ca = 0.3 for the case 7.5% w/w PVA, and Ca = 0.5 for the case 10% w/w PVA.

very low value of the interfacial tension at the interface between chloroform/DMPC and water. These high values of Ca partially account for the large deformations of the inner water phase. Moreover, the velocity profiles in the different aqueous phases in Figure 3 are expected to be significantly different from the profile in Figure 1 because of the modified viscosity contrast between the outer and the inner phases. Indeed, numerical work (for simple droplet flows) has already shown that the flow profile depends on the viscosity ratio between the inner and the outer phases.[36] As such, increasing the viscosity of the outer phase would naturally lead to a different stress field on the flowing droplets than having a viscosity ratio of unity. Here, both the oil shell and the core undergo deformation, which gradually increases until the tubes are extruded at the rear end, and eventually break up, as displayed in Figure 3 (see Videos 2−4). The extent of deformation by varying the concentration of PVA was quantified by plotting D (as defined previously) vs the position (x) in the channel (Figure S6a). The results show a linear and a gradual deformation of the DEs for a given concentration of PVA upon traveling in the channel with the highest deformation obtained for 10% PVA as deduced from the slopes of the deformation curves (Figure S6b). Upon increasing the concentration of PVA, which translates to an increase of the capillary number, the deformation increases as shown in Figure S6c. These results are in good agreement with previous reports in the literature where high capillary numbers were shown to induce deformation and breakup of simple or double-emulsion droplets.[25−30] The various experimental conditions and regimes observed in this study are summarized in the phase diagrams plotted in Figure S7. They show that a transition from deformation to tip streaming and breakup can occur when Ca reaches a value below ∼0.6. The deformation of double emulsions subjected to a shear flow was studied experimentally and using numerical simulations by Chen et al.,[26,27] who evidenced four types of breakup modes depending on the capillary number. A breakup via a mechanism based on capillary instability was reported for large capillary numbers as observed in this work. To identify what is being streamed behind the mother droplet, bright field and fluorescence images are acquired at different positions in the capillary tube for the case of 5% w/w PVA in the continuous phase. The higher intensity of red color at the rear of the drops shows that the phospholipids are accumulating at this position (Figure 4A2). At a distance downstream of the position where the tip streaming has initiated (Figure 4B2) the daughter droplets appear green in the fluorescent image, which indicates that they remain compartmentalized within the outer aqueous phase. The absence of the red signal stemming from the rhodamine B-labeled phospholipids in this case is ascribed to the low concentration in the thin oil shell encapsulating the daughter droplets, insufficient to be captured with the low exposure time used for the dynamic recordings.

At the exit of the microchannel the droplets were collected and analyzed by bright field and fluorescence microscopy at long exposure times. The bright field image (Figure 4C) shows the presence of monodisperse mother droplets with a size of around 250 μm and smaller droplets generated from the tip streaming with a size ranging from 5 to 30 μm. On the top of the mother droplets, small bubbles (dots) are observed which can be attributed to the evaporation of chloroform from the oil shell. The mother and daughter droplets both exhibit fluorescence signals from the fluorescein in the aqueous core and the rhodamine B-labeled phospholipids in the oil shell as shown by fluorescence microscopy, Figure 4D and 4E, respectively. These results demonstrate clearly that both types of droplets are compartments delimited from the external aqueous phase by a chloroform shell containing phospholipids and that the daughter droplets inherit from the encapsulated material as well as the oil/phospholipid material. This is also confirmed by the plot profile of the intensity of fluorescence of fluorescein and rhodamine (Figure 4F and 4G) across the mother and daughter droplets (indicated by arrows) measured using ImageJ.

To verify the formation of lipid membranes, we encapsulated fluorescein and 0.2 M sucrose in the inner core of the double emulsions (along with 2% w/w PVA) prior to tip streaming as previously described.[13,37] The resulting droplets were collected in a 2% w/w PVA solution (blank) or in 2% w/w PVA solution containing 50 μg/mL α-hemolysin. The latter spontaneously incorporates into the phospholipid membrane, forming narrow pores. The as-formed pores allow fluorescein to exit the droplet core due to the concentration gradient and water to enter from the exterior matrix due to an osmotic pressure gradient caused by the encapsulated sucrose which will cause the droplets to swell. After 15 min of incubation in the absence of α-hemolysin, an increase in the size of ∼1% is observed, lying within the statistical uncertainty, indicating that water does not cross the membrane from the outer to the inner phase. Also, no increase in the fluorescence intensity is observed in the external phase, indicating that no passage of fluorescein from the inner phase to the external phase has occurred (most right image, Figure 5A). However, an incubation time of 15 min in the α-hemolysin solution resulted in an increase in fluorescence intensity outside the droplets (most right image, Figure 5B) and an increase of ∼8% in size for mother and daughter droplets with the average size of the mother droplets passing from 256 ± 14.5 μm initially (57 ± 18 μm for daughter droplets) to a final size of 279 ± 16 μm (62 ± 20 μm for daughter droplets) as illustrated by the histograms in Figure 5.

https://doi.org/10.1021/acs.langmuir.1c00827
Langmuir 2021, 37, 7442−7448

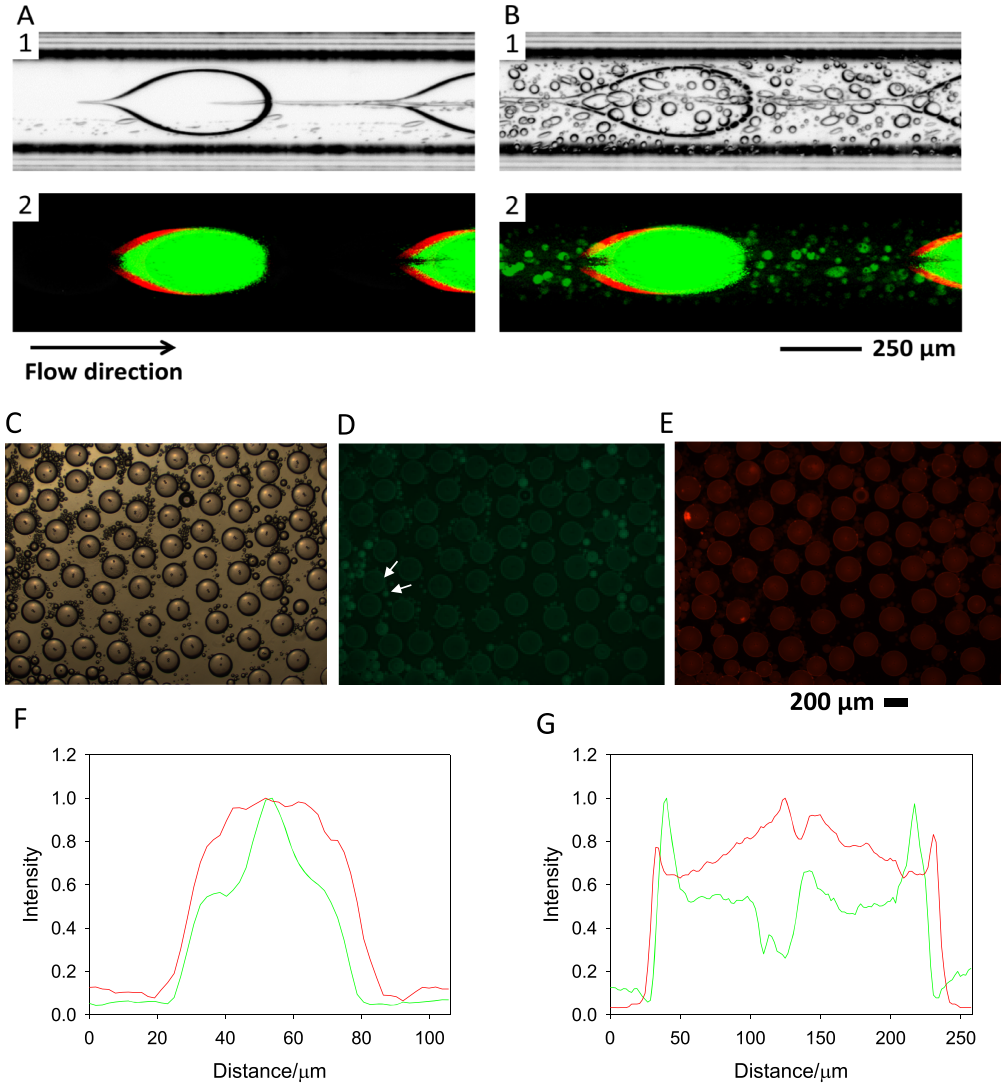

Figure 4. Bright field (1) and fluorescence (2) images (A) prior to tip streaming and (B) at a position where tip streaming has been initiated. Contrast of the green color channel was enhanced to make the daughter droplets appear clearly in image B2. Flow rates applied: Q_1 (H_2O/2% w/w PVA and 0.02% w/w fluorescein) = 4.17×10^{-4} cm^3 s^{-1}, Q_2 (chloroform/1% w/w DMPC and 0.02% w/w rhodamine B-labeled phospholipids) = 1.67×10^{-4} cm^3 s^{-1}, and Q_3 (H_2O/5% w/w PVA) = 1.67×10^{-4} cm^3 s^{-1}. Ca = 0.10. See also Videos 5 and 6. (C, D, and E) Bright field image, fluorescein encapsulated in the core, and rhodamine B-labeled phospholipids in the oil shell, respectively, of mother and daughter droplets collected on a glass slide. Normalized fluorescence intensity plot profiles for fluorescein (green line) and rhodamine B-labeled phospholipids (red line) on daughter droplet (F; white arrow) and mother droplet (G; white arrow).

These results provide evidence that all of the obtained compartments are phospholipid vesicles.

CONCLUSIONS

In summary, the dynamic behavior of w/o/w double emulsions generated in a microfluidic device using the phospholipid 1,2-dimyristoyl-*sn*-glycero-3-phosphocholine (DMPC) as a phospholipid and chloroform as the oil phase is reported in this manuscript. We show that using such formulation, the dynamic behavior of the double emulsions under flow gives rise to strong deformation and tip streaming. Although such a behavior is well known for droplets formulated using surfactants, it has not been reported neither with double emulsions nor with phospholipids. When the double emulsions were generated using the same composition and viscosity in the core and the outer continuous flowing phase, the concentration of DMPC had a strong impact on the nature and degree of deformation of the middle phase: the shape of the core remained practically unperturbed, while increasing the DMPC concentration resulted in the double emulsions adapting a pear-like shape. Indeed, the higher the DMPC concentration destabilized faster and displayed strong tip streaming at the rear of the flowing droplets. In this situation it is possible that stacking of DMPC bilayers was less efficient at higher lipid concentration due to increasing disorder in multiple layers with resulting unfavorable compartmentalization. The tubes that thus emerged were gradually extruded at the rear of the double emulsions. They eventually pinch off at the tube extremity, in typical form of tip streaming, as smaller (daughter) compartments were released upon evaporation of chloroform in the form of phospholipid vesicles. The presence of daughter droplets due to tip streaming may be considered as the main disadvantage of this method for the purpose of encapsulation. However, in other cases it can be seen as an advantage to generate very small phospholipid vesicles, which may eventually be expelled from the mother structures, as it

https://doi.org/10.1021/acs.langmuir.1c00827
Langmuir 2021, 37, 7442−7448

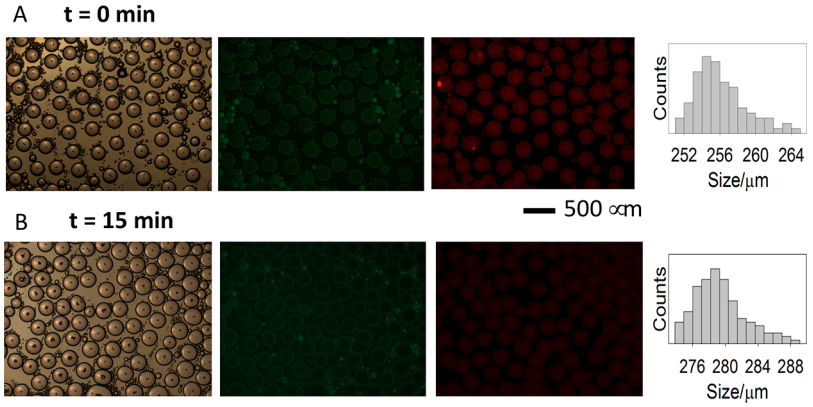

Figure 5. Images showing the effect of membrane-incorporated α-hemolysin (from left to right: bright field, rhodamine B fluorescence, and fluorescein fluorescence). Images recorded immediately after addition of α-hemolysin (A) and after 15 min of incubation with α-hemolysin (B) in a 2% w/w PVA matrix. Droplets were generated using the same conditions as described for Figure 4. Histograms display the size increase (swelling) induced by the diffusion of water into the core of the vesicles.

happens for instance in cell budding. Centrifugation can be used to separate the vesicles by size or other methods depending on the encapsulated material, such as magnetophoresis for magnetic vesicles. Also, our system may serve as a model to mimic the generation of extravesicles from cells which can be also used for studying interesting steps in the cell cycle.[38,39] In the future, we would like investigate more in detail the mechanical and fluid-dynamical aspects of this phenomenon by applying other stimulus which can affect the surface tension, including light, using photoactivatable molecules (phospholipids, surfactants)[40] and magnetic fields[41] (by encapsulation of magnetic particles) on inducing and manipulating the tip streaming under a hydrodynamic flow.

■ ASSOCIATED CONTENT

Supporting Information

The Supporting Information is available free of charge at https://pubs.acs.org/doi/10.1021/acs.langmuir.1c00827.

Videos on DE generation (ZIP)

Microfluidic generation of the double emulsions, viscosity measurements, surface tension measurements, fluorescence and bright field images, PVA viscosity effect, phase diagrams (PDF)

■ AUTHOR INFORMATION

Corresponding Author

Ali Abou-Hassan − *Sorbonne Université, CNRS UMR 8234, Laboratoire PHysico-chimie des Électrolytes et Nanosystèmes InterfaciauX, PHENIX, F-75005 Paris, France;* orcid.org/0000-0002-9070-1024; Email: ali.abou_hassan@sorbonne-universite.fr

Authors

Kristian Torbensen − *Sorbonne Université, CNRS UMR 8234, Laboratoire PHysico-chimie des Électrolytes et Nanosystèmes InterfaciauX, PHENIX, F-75005 Paris, France;* Present Address: Université de Paris, Laboratoire d'Electrochimie Moléculaire, UMR CNRS-P7 7591, 75205 Paris, Cedex 13, France

Charles N. Baroud − *Physical Microfluidics & Bioengineering, Institut Pasteur, 75015 Paris, France*

Sandra Ristori − *Chemistry Department & CSGI, University of Florence, 50019 Sesto Fioretino, Italy*

Complete contact information is available at: https://pubs.acs.org/10.1021/acs.langmuir.1c00827

Author Contributions

The manuscript was written through contributions of all authors. All authors have given approval to the final version of the manuscript.

Notes

The authors declare no competing financial interest.

■ ACKNOWLEDGMENTS

K.T. and A.A.-H. acknowledge F. Brochard Wyart and Patricia Bassereau, Institut Curie and Sorbonne University, for fruitful discussions and the doctoral school ED 398 Chimie Physique et Chimie Analytique de Paris Centre for funding.

■ REFERENCES

(1) Shang, L.; Cheng, Y.; Zhao, Y. Emerging Droplet Microfluidics. *Chem. Rev.* **2017**, *117*, 7964−8040.

(2) Suea-Ngam, A.; Howes, P. D.; Srisa-Art, M.; deMello, A. J. Droplet Microfluidics: From Proof-of-Concept to Real-World Utility? *Chem. Commun.* **2019**, *55*, 9895−9903.

(3) Kane, R. S.; Stroock, A. D.; Li Jeon, N.; Ingber, D. E.; Whitesides, G. M. In *Optical Biosensors*; Ligler, F. S., Taitt, C. A. R., Eds.; Elsevier Science: Amsterdam, 2002; Chapter 18 (Soft Lithography and Microfluidics), pp 571−595.

(4) Utada, A. S.; Lorenceau, E.; Link, D. R.; Kaplan, P. D.; Stone, H. A.; Weitz, D. A. Monodisperse Double Emulsions Generated from a Microcapillary Device. *Science* **2005**, *308*, 537−541.

(5) Abou-Hassan, A.; Dufrêche, J.-F.; Sandre, O.; Mériguet, G.; Bernard, O.; Cabuil, V. Fluorescence Confocal Laser Scanning Microscopy for Ph Mapping in a Coaxial Flow Microreactor: Application in the Synthesis of Superparamagnetic Nanoparticles. *J. Phys. Chem. C* **2009**, *113*, 18097−18105.

(6) Mashaghi, S.; Abbaspourrad, A.; Weitz, D. A.; van Oijen, A. M. Droplet Microfluidics: A Tool for Biology, Chemistry and Nanotechnology. *TrAC, Trends Anal. Chem.* **2016**, *82*, 118−125.

(7) Ferraro, D.; Lin, Y.; Teste, B.; Talbot, D.; Malaquin, L.; Descroix, S.; Abou-Hassan, A. Continuous Chemical Operations and Modifications on Magnetic γ-Fe_2O_3 Nanoparticles Confined in Nanoliter Droplets for the Assembly of Fluorescent and Magnetic SiO_2@γ-Fe_2O_3. *Chem. Commun.* **2015**, *51*, 16904−16907.

(8) Baroud, C. N.; Gallaire, F.; Dangla, R. Dynamics of Microfluidic Droplets. *Lab Chip* **2010**, *10*, 2032−2045.

(9) Casadevall i Solvas, X.; deMello, A. Droplet Microfluidics: Recent Developments and Future Applications. *Chem. Commun.* **2011**, *47*, 1936−1942.
(10) Ding, S.; Serra, C. A.; Vandamme, T. F.; Yu, W.; Anton, N. Double Emulsions Prepared by Two-Step Emulsification: History, State-of-the-Art and Perspective. *J. Controlled Release* **2019**, *295*, 31−49.
(11) Bhattacharya, A.; Devaraj, N. K. Tailoring the Shape and Size of Artificial Cells. *ACS Nano* **2019**, *13*, 7396−7401.
(12) Okushima, S.; Nisisako, T.; Torii, T.; Higuchi, T. Controlled Production of Monodisperse Double Emulsions by Two-Step Droplet Breakup in Microfluidic Devices. *Langmuir* **2004**, *20*, 9905−9908.
(13) Arriaga, L. R.; Datta, S. S.; Kim, S.-H.; Amstad, E.; Kodger, T. E.; Monroy, F.; Weitz, D. A. Ultrathin Shell Double Emulsion Templated Giant Unilamellar Lipid Vesicles with Controlled Microdomain Formation. *Small* **2014**, *10*, 950−956.
(14) Ho, K. K. Y.; Lee, L. M.; Liu, A. P. Mechanically Activated Artificial Cell by Using Microfluidics. *Sci. Rep.* **2016**, *6*, 32912.
(15) Tomasi, R.; Noel, J.-M.; Zenati, A.; Ristori, S.; Rossi, F.; Cabuil, V.; Kanoufi, F.; Abou-Hassan, A. Chemical Communication between Liposomes Encapsulating a Chemical Oscillatory Reaction. *Chem. Sci.* **2014**, *5*, 1854−1859.
(16) Habault, D.; Dery, A.; Leng, J.; Lecommandoux, S.; Le Meins, J.-F.; Sandre, O. Droplet Microfluidics to Prepare Magnetic Polymer Vesicles and to Confine the Heat in Magnetic Hyperthermia. *IEEE Trans. Magn.* **2013**, *49*, 182−190.
(17) Seth, A.; Béalle, G.; Santanach-Carreras, E.; Abou-Hassan, A.; Ménager, C. Design of Vesicles Using Capillary Microfluidic Devices: From Magnetic to Multifunctional Vesicles. *Adv. Mater.* **2012**, *24*, 3544−3548.
(18) Wang, W.; Zhang, M.-J.; Xie, R.; Ju, X.-J.; Yang, C.; Mou, C.-L.; Weitz, D. A.; Chu, L.-Y. Hole-Shell Microparticles from Controllably Evolved Double Emulsions. *Angew. Chem.* **2013**, *125*, 8242−8245.
(19) Zhang, Y.; Ho, Y.-P.; Chiu, Y.-L.; Chan, H. F.; Chlebina, B.; Schuhmann, T.; You, L.; Leong, K. W. A Programmable Microenvironment for Cellular Studies Via Microfluidics-Generated Double Emulsions. *Biomaterials* **2013**, *34*, 4564−4572.
(20) Torbensen, K.; Rossi, F.; Pantani, O. L.; Ristori, S.; Abou-Hassan, A. Interaction of the Belousov-Zhabotinsky Reaction with Phospholipid Engineered Membranes. *J. Phys. Chem. B* **2015**, *119*, 10224−10230.
(21) Rossi, F.; Zenati, A.; Ristori, S.; NoÎl, J.-M.; Cabuil, V.; Kanoufi, F.; Abou-Hassan, A. Activatory Coupling among Oscillating Droplets Produced in Microfluidic Based Devices. *Int. J. Unconv. Comput.* **2015**, *11*, 23−36.
(22) Budroni, M. A.; Torbensen, K.; Pantani, O. L.; Ristori, S.; Rossi, F.; Abou-Hassan, A. Microfluidic Compartmentalization of Diffusively Coupled Oscillators in Multisomes Induces a Novel Synchronization Scenario. *Chem. Commun.* **2020**, *56*, 11771−11774.
(23) Eggleton, C. D.; Tsai, T.-M.; Stebe, K. J. Tip Streaming from a Drop in the Presence of Surfactants. *Phys. Rev. Lett.* **2001**, *87*, 048302.
(24) Anna, S. L.; Bontoux, N.; Stone, H. A. Formation of Dispersions Using "Flow Focusing" in Microchannels. *Appl. Phys. Lett.* **2003**, *82*, 364−366.
(25) Zhao, C.-X.; Middelberg, A. P. J. Two-Phase Microfluidic Flows. *Chem. Eng. Sci.* **2011**, *66*, 1394−1411.
(26) Hua, H.; Shin, J.; Kim, J. Dynamics of a Compound Droplet in Shear Flow. *Int. J. Heat Fluid Flow* **2014**, *50*, 63−71.
(27) Chen, Y.; Liu, X.; Shi, M. Hydrodynamics of Double Emulsion Droplet in Shear Flow. *Appl. Phys. Lett.* **2013**, *102*, 051609.
(28) Chen, Y.; Liu, X.; Zhao, Y. Deformation Dynamics of Double Emulsion Droplet under Shear. *Appl. Phys. Lett.* **2015**, *106*, 141601.
(29) Ma, S.; Huck, W. T. S.; Balabani, S. Deformation of Double Emulsions under Conditions of Flow Cytometry Hydrodynamic Focusing. *Lab Chip* **2015**, *15*, 4291−4301.
(30) Zhou, C.; Yue, P.; Feng, J. J. Formation of Simple and Compound Drops in Microfluidic Devices. *Phys. Fluids* **2006**, *18*, 092105.
(31) Tao, J.; Song, X.; Liu, J.; Wang, J. Microfluidic Rheology of the Multiple-Emulsion Globule Transiting in a Contraction Tube through a Boundary Element Method. *Chem. Eng. Sci.* **2013**, *97*, 328−336.
(32) Chen, H.; Li, J.; Shum, H. C.; Stone, H. A.; Weitz, D. A. Breakup of Double Emulsions in Constrictions. *Soft Matter* **2011**, *7*, 2345−2347.
(33) Torbensen, K.; Abou-Hassan, A. Easy-to-Assemble and Adjustable Coaxial Flow-Focusing Microfluidic Device for Generating Controllable Water/Oil/Water Double Emulsions: Toward Templating Giant Liposomes with Different Properties. *J. Flow Chem.* **2015**, *5*, 234−240.
(34) Ajaev, V. S.; Homsy, G. M. Modeling Shapes and Dynamics of Confined Bubbles. *Annu. Rev. Fluid Mech.* **2006**, *38*, 277−307.
(35) Taylor, G. I. The Formation of Emulsions in Definable Fields of Flow. *Proc. R. Soc. London, Ser. A* **1934**, *146*, 501−523.
(36) Hodges, S. R.; Jensen, O. E.; Rallison, J. M. The Motion of a Viscous Drop through a Cylindrical Tube. *J. Fluid Mech.* **1999**, *501*, 279−301.
(37) Bao, P.; Paterson, D. A.; Peyman, S. A.; Jones, J. C.; Sandoe, J. A. T.; Gleeson, H. F.; Evans, S. D.; Bushby, R. J. Production of Giant Unilamellar Vesicles and Encapsulation of Lyotropic Nematic Liquid Crystals. *Soft Matter* **2021**, *17*, 2234−2241.
(38) Mathieu, M.; Martin-Jaular, L.; Lavieu, G.; Théry, C. Specificities of Secretion and Uptake of Exosomes and Other Extracellular Vesicles for Cell-to-Cell Communication. *Nat. Cell Biol.* **2019**, *21*, 9−17.
(39) Liu, Q.; Bi, C.; Li, J.; Liu, X.; Peng, R.; Jin, C.; Sun, Y.; Lyu, Y.; Liu, H.; Wang, H.; Luo, C.; Tan, W. Generating Giant Membrane Vesicles from Live Cells with Preserved Cellular Properties. *Research* **2019**, *2019*, 6523970.
(40) Diguet, A.; Li, H.; Queyriaux, N.; Chen, Y.; Baigl, D. Photoreversible Fragmentation of a Liquid Interface for Micro-Droplet Generation by Light Actuation. *Lab Chip* **2011**, *11*, 2666−2669.
(41) Rigoni, C.; Fresnais, J.; Talbot, D.; Massart, R.; Perzynski, R.; Bacri, J. C.; Abou-Hassan, A. Magnetic Field-Driven Deformation, Attraction, and Coalescence of Nonmagnetic Aqueous Droplets in an Oil-Based Ferrofluid. *Langmuir* **2020**, *36*, 5048−5057.

https://doi.org/10.1021/acs.langmuir.1c00827
Langmuir 2021, 37, 7442−7448